*35th EPS Conference on Plasma Phys. Hersonissos, 9 - 13 June 2008 ECA Vol.**32D**, P-5.156 (2008)*

High-res simulations of interstellar MHD turbulence – Spatial structure and statistics

R. Kissmann[1], J. Kleimann[2], H. Fichtner[3], R. Grauer[4]

[1] *Institut für Astronomie und Astrophysik, Universität Tübingen, Tübingen, Germany*

[2] *Nordlys Observatoriet, Universitetet i Tromsø, Tromsø, Norway*

[3] *Theoretische Physik IV, Ruhr-Universität Bochum, Bochum, Germany*

[4] *Theoretische Physik I, Ruhr-Universität Bochum, Bochum, Germany*

Introduction

The plasma of the interstellar medium (ISM) is nowadays considered to be in a turbulent state on many observable scales. We use numerical MHD to investigate the properties of this turbulent plasma, focusing on molecular clouds (MCs) and the diffuse interstellar gas (DIG). We present an analysis of the spatial plasma distribution, and some key statistical properties of the medium thus simulated.

The physical model

The single-fluid equations of ideal MHD

$$\frac{\partial \rho}{\partial t} + \nabla \cdot (\rho \mathbf{u}) = 0 \tag{1}$$

$$\frac{\partial (\rho \mathbf{u})}{\partial t} + \nabla \cdot \left[\rho \mathbf{u}\mathbf{u} + \left(p + \frac{B^2}{2\mu_0} \right) \underline{\mathbf{1}} - \frac{1}{\mu_0} \mathbf{B}\mathbf{B} \right] = 0 \tag{2}$$

$$\frac{\partial \mathbf{B}}{\partial t} + \nabla \cdot (\mathbf{u}\mathbf{B} - \mathbf{B}\mathbf{u}) = 0 \tag{3}$$

$$\frac{\partial e}{\partial t} + \nabla \cdot \left(\left(e + p + \frac{B^2}{2\mu_0} \right) \mathbf{u} - \frac{1}{\mu_0} (\mathbf{u} \cdot \mathbf{B}) \mathbf{B} \right) = n_{\mathrm{H}} \Gamma - (n_{\mathrm{H}})^2 \Lambda \tag{4}$$

whose energy source terms represent heating (Γ) and cooling functions (Λ), are solved numerically using an implementation of a Riemann-solver free, semi-discrete central scheme [4] employing TVD reconstruction and a minmod limiter. The $\nabla \cdot \mathbf{B} = 0$ condition is ensured using a constrained transport method [2]. The computational domain consists of a cube of side length 40 pc with periodic boundary conditions.

Starting from an initially homogeneous configuration (with $\mathbf{B}_{t=0} = B_0\, \mathbf{e}_x$), the turbulence is driven at large scales by incompressible velocity fluctuations with random amplitudes (following a power spectrum $E(k) \propto k^{-1}$), which are of the same magnitude as the energy input by supernova explosions.

Due to their very different physical nature, molecular clouds (MDs) and the DIG are modelled with different parameters (see Table 1), and with a different treatment of their energy budget.

	MC	DIG
Ionization $x_0 = n_e/n_H$	0.01	0.1
Average density n_H [m^{-3}]	10^8	10^6
Initial temperature T_0 [K]	56	1000
Velocity normalization $v_0 = c_s$ [m/s]	480	2000
Spatial Resolution N	512^3	256^3
resulting grid size Δx [pc]	0.08	0.16

Table 1: Parameters for the MC and DIG application runs, respectively.

Target I: Molecular Clouds

Since a MC is shielded from the interstellar FUV radiation field, $\Gamma = 0 = \Lambda$, and the energy equation (4) can be discarded in favor of the closure relation

$$p = \begin{cases} p_0 \, (\rho/\rho_0)^\gamma & : \quad \gamma \neq 1 \\ (c_s)^2 \, \rho & : \quad \gamma = 1 \end{cases} \qquad (5)$$

where $c_s = \sqrt{(k_B \, T_0)/m_0}$ is the isothermal sound speed, and γ denotes the adiabatic exponent. The resulting density structures yield sharper gradients for the isothermal case (see Fig. 1) when compared to adiabatic runs (not shown).

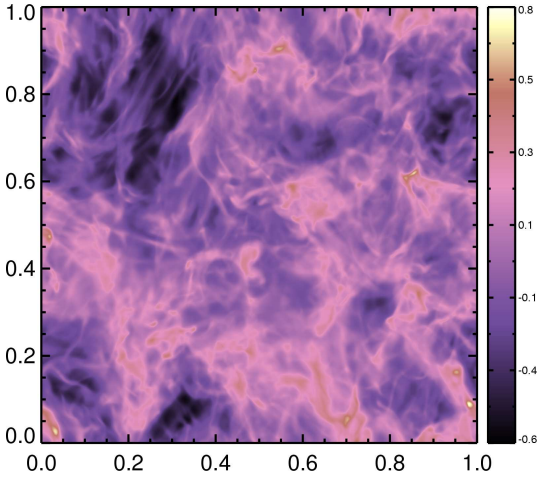

Figure 1: Dispersion measure $\int_0^L n_e \, ds$ for an isothermal run.

Turbulence statistics

Looking at the density power spectrum (Fig. 2), we see that the isothermal case has more energy at large wavenumbers. The fluctuations in the inertial range also differ. For the velocity fluctuations, however, the spectrum and also the resulting structure functions are virtually identical for both cases, which lends support to the She-Leveque model [6].

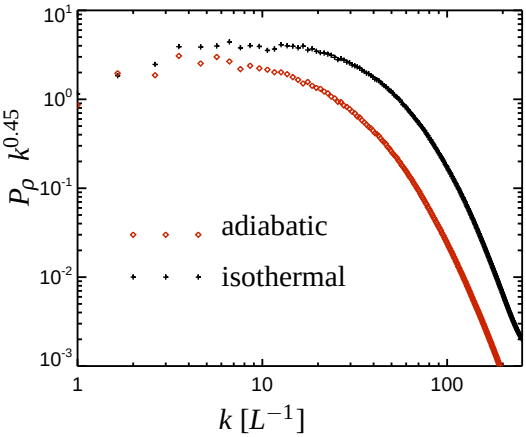

Figure 2: Normalized power spectrum, multiplied with $k^{0.45}$ vs. wave number k for $\gamma = 1$ (black) and $\gamma = 5/3$ (red).

Target II: The diffuse interstellar gas

The DIG, which is heated by FUV photons, requires full treatment with Eq. (4), including realistic heating and cooling functions. Heating occurs

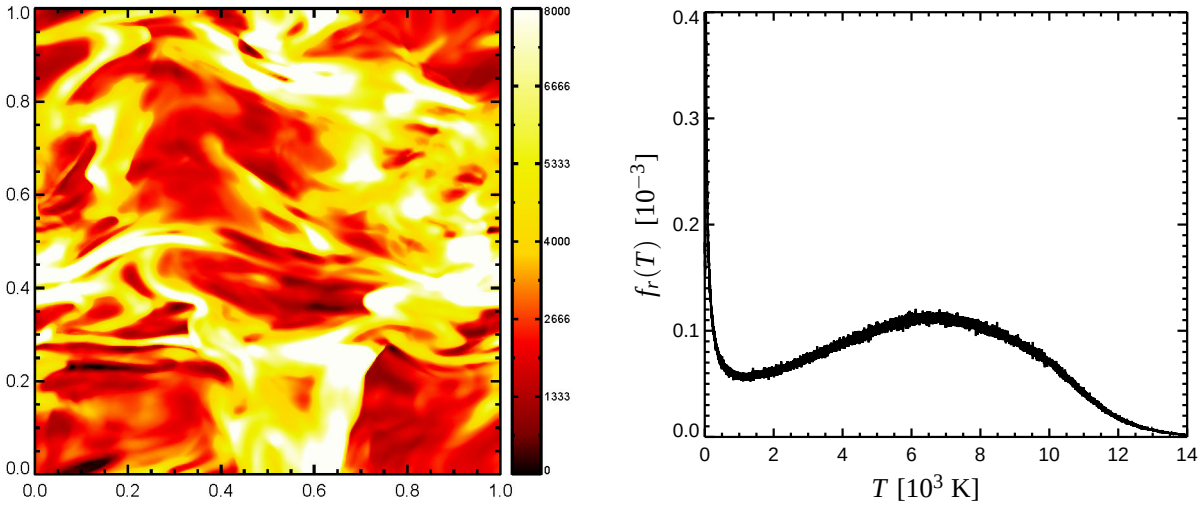

Figure 3: Temperature map in a plane slicing the volume (left), and the temperature distribution function $f_r(T)$ with respect to the entire domain (right).

via external FUV radiation incident upon dust grains [1, 7]. We use

$$\Gamma(n_\mathrm{e}, T)\, n_\mathrm{H} = \Gamma_0\, n_\mathrm{e}\, \varepsilon(T, n_\mathrm{e}) \tag{6}$$

with $\Gamma_0 = 1.7 \cdot 10^{-25}$ J m^{-3} s^{-1} and $\varepsilon(T, n_\mathrm{e})$, the fraction of absorbed FUV radiation, given by [1]. For cooling, let $i \in \{\mathrm{C}, \mathrm{N}, \mathrm{O}, \mathrm{Si}, \mathrm{S}, \mathrm{Fe}\}$ with abundances X_i. Then for $T < 10^{4.2}$ K we use

$$\Lambda(T)\, n_\mathrm{H} = \sum_i \left[x_0\, \lambda_\mathrm{e}(X_i, T) + \lambda_\mathrm{H}(X_i, T)\right]\, n_i \tag{7}$$

with $\lambda_{\mathrm{e,H}}(X_i, T)$ taken from [5]. For $T > 10^{4.2}$ K, the parameterisation due to [3] was applied. From these heating and cooling functions (6, 7), we can compute a pressure versus density curve for the thermal equilibrium (not shown). This curve indicates the presence of two stable regimes, separated by a thermally unstable range at approximately $n_\mathrm{H}/(10^6\ \mathrm{m}^{-3}) \in [0.4,\ 5.0]$.

The two-phase medium

Our simulations reproduce a warm phase (several 10^3 K), separated by much cooler clouds (< 500 K), see Fig. 3. This is in agreement with observations, and is also consistent with the presence of two distinct phases in the pressure-density equilibrium curve mentioned above. In our simulations, we find a significant amount of gas in the unstable regime.

Getting $\langle B_\parallel \rangle$ from rotation / dispersion measure?

Values of the interstellar magnetic field are often inferred from the ratio of rotation and dispersion measure. Fig. 4 compares the result so obtained with the actual line-of-sight integral. This highlights the inferior agreement of both data sets, which is caused by the highly inhomogeneous distribution of matter in the simulation.

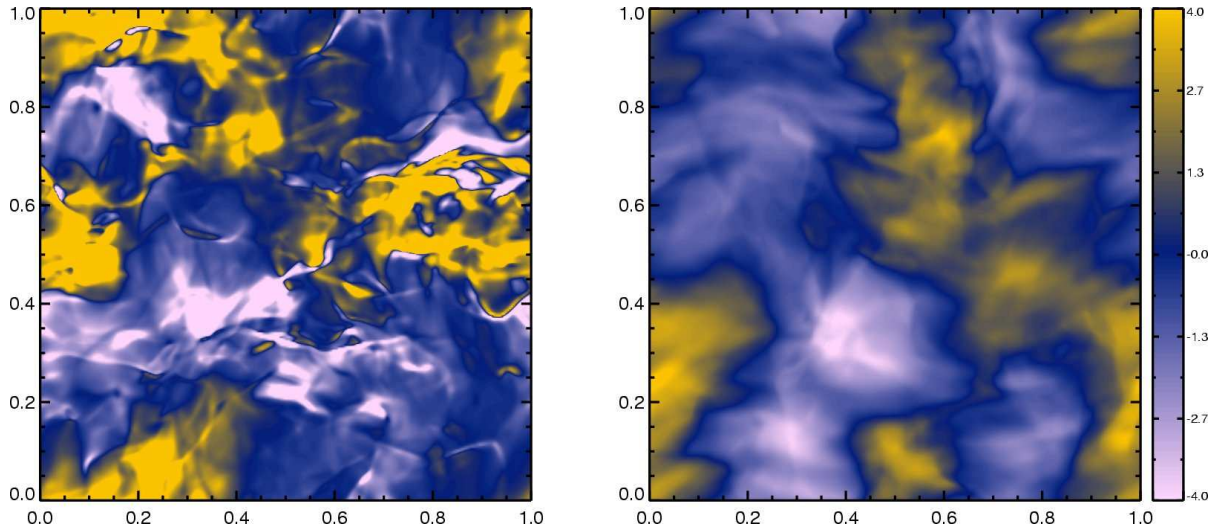

Figure 4: Density-weighted average of $B_{\|}$, as would be inferred from RM/DM (left), compared to the actual line-of-sight integral $\left(\int_0^L B_{\|}\,\mathrm{d}s\right) \Big/ L$ (right). The discrepancy with respect to $\left(\int_0^L n_\mathrm{e} B_{\|}\,\mathrm{d}s\right) \Big/ \left(\int_0^L n_\mathrm{e}\,\mathrm{d}s\right)$ is very obvious.

Summary and Conclusions

We have presented MHD simulations of the ISM, focusing on molecular clouds (isothermal and adiabatic) and the DIG (using the full energy balance with realistic heating and cooling functions). For the MCs, we found that a change in the equation of state (from adiabatic to isothermal) yields stronger local gradients and more power at high wave numbers of the density fluctuation spectrum. For the DIG, we could clearly identify two phases (cold and warm), in accord with observations. A direct comparison of the line-of-sight $B_{\|}$ integral with its value as inferred from rotation/ dispersion mesaure casts doubts on the applicability of the latter method in cases where strong density gradients are present.

References

[1] E.L.O. Bakes, A.G.G.M. Thielens, *ApJ* **427**, 822 (1994)

[2] C.R. Evans, J. F. Hawley, *ApJ* **332**, 659 (1998)

[3] J.P.E. Gerritsen, V. Icke, *A&A* **325**, 972 (1997)

[4] A. Kurganov, S. Noelle, G. Petrova, SIAM J. Sci. Comp. **23**, 707 (2001)

[5] M.V. Penston, *ApJ* **162**, 771 (1970)

[6] Z.-S. She, E. Leveque, *PhRvL* **3**, 336 (1994)

[7] M.G. Wolfire and 4 co-authors, *ApJ* **443**, 152 (1995)